

Optimized design and experiment on ring mold pelletizer for producing biomass fuel pellets

Gao Wei^{1,2}, Lope G Tabil², Zhao Rongfei^{3*}, Liu Dejun¹

(1. College of Engineering, Shenyang Agricultural University, Shenyang 110866, China;

2. Department of Chemical and Biological Engineering, University of Saskatchewan, Saskatoon S7N 5A9, Canada;

3. College of Water Conservancy, Shenyang Agricultural University, Shenyang 110866, China)

Abstract: The forming process of biomass fuel pellets using a ring mold pelletizer was analyzed, optimized, tested and evaluated in this study. The effects of stress amplitude and the stress ratio on the fatigue failure of the ring mold under 4-, 3-, and 2-roller designs were investigated. Depending on the calculation of stress amplitude acting on the ring mold, the 4-roller design was chosen for having the smallest value of stress amplitude in this condition. After determining the main design parameters, a three-dimensional model of the ring mold pelletizer was established based on the Pro/Engineer software, and the model was transferred into ADAMS software through Mechanism/Pro which is a dedicated interface software. The ADAMS software was used to run simulations. In order to obtain the highest efficiency and the lowest power consumption, the optimal result was the 4-roller design. Finally, a prototype of the ring mold pelletizer with four rollers was designed and manufactured for biomass fuel pellet production. Corn stover biomass was used as material for experimental manufacturing of fuel pellets. Test and evaluation showed that the optimized pellet durability was 99.79% with ground corn stover particles passing a screen size of 1.97 mm, moisture content of 21.2% w.b. and a material moisture conditioning time of 3.82 h. Pellets formed in the prototype ring mold pelletizer using corn stover had acceptable durability according to European standards.

Keywords: biomass pellet, ring mold pelletizer, optimized design, biofuel, corn stover, Pro/Engineer, Adams, pellet durability

DOI: 10.3965/j.ijabe.20160903.2074

Citation: Gao W, Tabil L G, Zhao R F, Liu D J. Optimized design and experiment on ring mold pelletizer for producing biomass fuel pellets. *Int J Agric & Biol Eng*, 2016; 9(3): 57–66.

1 Introduction

Fuel pellets can be developed from biomass sources utilizing pelleting equipment currently available. The design of the pelleting equipment can potentially be

improved and optimized so as to reduce pelleting cost^[1,2]. The emissions from biomass pellet combustion in terms of SO₂, NO_x and other pollutants is far below the emission standards for air pollutants^[3-5]. Pelleting using a ring mold pelletizer does not require external heating nor additives or binders. It relies on frictional heat, resulting in the softening of the biomass particles, and extrusion molding, resulting in the compaction of particles to a certain density and shape. It is an ideal forming process for biomass pellet production^[6,7]. Equipment design involves a long research and development cycle and a high testing cost. This reality restricts the application and development of ring mold pelletizer technology. Wang et al.^[8] established biomass parameters of the ring mold model by SolidWorks software; they also conducted numerical analysis of the ring mold with different structural parameters using

Received date: 2015-07-24 **Accepted date:** 2016-02-16

Biographies: Gao Wei, PhD, Lecturer, research interests: biofuels and biomass preprocessing, Email: snowwei28@126.com; Lope G Tabil, PhD, Professor, research interests: biomass preprocessing, bioenergy, biofuels, and value-added processing of agricultural crops, Email: lope.tabil@usask.ca; Liu Dejun, PhD, Associate Professor, research interests: agricultural products harvest and process, Email: ldjldj@126.com.

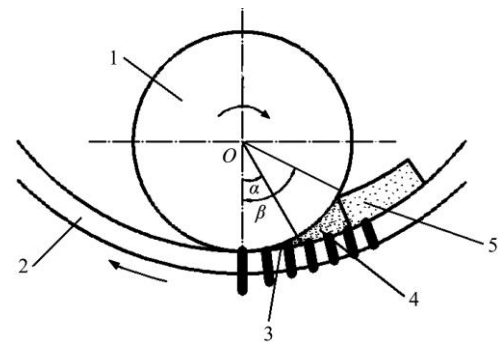
***Corresponding author:** Zhao Rongfei, PhD, Lecturer, research interests: agricultural soil and water engineering. College of Water Conservancy, Shenyang Agricultural University, Mailing address: No. 120 Donglin Road Shenyang, Liaoning. Tel: 15940146713. Email: xngwrf@163.com.

CosmosWorks software and they obtained the fatigue life of the ring mold under different conditions. Liu et al.^[9] conducted numerical analysis of the relationship between the basic size of the ring mold die and the strength of biomass using ANSYS software and obtained the best raw material particles forming effect when the die aspect ratio was around 5:1 (length: diameter). Abubakre et al.^[10] analyzed the relationship between the energy expenditure and the die size of a prototype by manufacturing test and reported that the efficiency increased with increase in the die size. Tu et al.^[11] established a solid model of biomass plane-die briquetting machine by UG software and imported the model into the software ADAMS/View module to simulate the process and reported that the main spindle bearing torque increased along with the increase of the roller pressure. The objective of this work was to design a ring mold pelletizer by modeling using the Pro/Engineer 3D software. The Adams software was used for the motion simulation analysis of high wear and pressure parts of the pelletizer. The designed ring mold pelletizer was fabricated and tested. Test and evaluation were undertaken: (1) to determine the relationship between biomass moisture content, particle size, and moisture conditioning time on pellet durability; and (2) to optimize the material and processing parameters for durability of biomass pellets.

2 Working principle and molding process

The ring mold pelletizer is composed of a power unit, a deceleration unit and the main body. The motor provides power to drive the rotating ring mold. The deceleration unit connects the motor to the shaft and the coupling; it has a reducer to control speed and increase the torque. The main body includes a screw conveyor, rollers, a ring mold, a roller plate and accessory parts. During rotation, extrusion pressure is generated between the ring mold and rollers, so that the particles of the biomass are shaped into a densified product (pellet). To form pellets, the biomass particles go through the feed zone, then compressed in the compression deformation zone and finally, the particles are extruded into the extrusion forming zone. The pellet formation process is

shown in Figure 1.



1. Roller 2. Ring mold 3. Extrusion forming zone 4. Compression deformation zone 5. Feed zone

α is the angle of extrusion forming zone, rad; β is the angle of whole compression deformation zone, rad.

Figure 1 Pellet formation process of particles in a ring mold

In the feed zone, the biomass is not affected by external mechanical forces, but it is subjected to centrifugal force produced by the high-speed rotation of the ring mold conveying the biomass to the deformation zone. In the compression deformation zone, with the rotation of ring mold and rollers, the material enters the nip. By the pressing action of rollers, the gap between the particles is gradually reduced, compressing the biomass particles, resulting in deformation and density increase. In the extrusion forming zone, the gap between the mold and rollers becomes smaller. The extrusion pressure increases rapidly, the biomass particles are pressed into the ring mold die. In the extrusion forming zone, the particles in the ring mold die is subjected to axial extrusion pressure to overcome the frictional pressure in the die wall and to extrude the formed pellet out of the die.

3 Three-dimensional solid modeling

3.1 Design parameters

The transmission ratios of the two stage cylindrical gear reducer were $i_1=4.6$ and $i_2=3.5$ for the first stage and second stage, respectively. Belt drive ratio was $i_3=2$. Table 1 lists the design specifications of the motor used in the pelletizer.

The spindle speed is given as:

$$n_s = n_m / i_1 i_2 i_3 = 1460 / (4.6 \times 3.5 \times 2) = 45.4 \text{ r/min} \quad (1)$$

where, n_s is rotational speed of spindle, r/min; n_m is rotational speed of the motor, r/min.

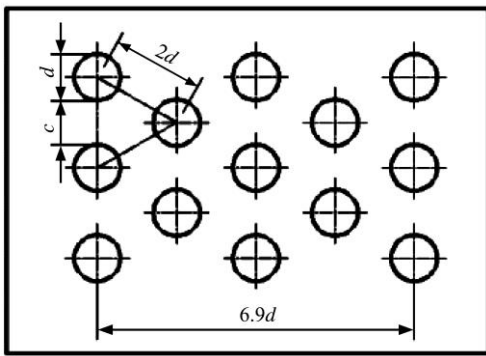
Table 1 Design specification of the motor

| Model and Manufacturer | Rated power /kW | Rotational speed/r min ⁻¹ | Efficiency /% |
|--|-----------------|--------------------------------------|---------------|
| Y160L-4 Shanghai Shenyue Electrical Co., Ltd. Daxi, Wenling, Zhejiang, China | 15 | 1460 | 88.5 |

3.2 Design of the main parts

3.2.1 Ring mold

The material selected for the ring mold was high chromium alloy steel. The tensile strength was equal or greater than 980 MPa. After heat treatment, the surface hardness was similar to that of 58-62HRC steel. The hole was straight, for simple processing and is applicable to a wide range of particles. The die holes were arranged as equilateral triangle (Figure 2), ensuring a uniform pressure distribution in the ring mold and reducing the breakage of parts.



Note: *d* is the diameter of die holes in the ring mold, mm; *c* is the smallest distance of two adjoining die holes in the ring mold, mm.

Figure 2 Arrangement of die holes in the ring mold

The inner diameter of the ring mold is:

$$D = \frac{60v}{\pi n_s} \tag{2}$$

where, *D* is the inner diameter of the ring mold, mm; *v* is the linear speed of the ring mold, for the machine selected, *v*=850 mm/s.

The thickness of the ring mold should consider not only the die effective length and intensity (die wall compressive stress), but also the die diameter and material (particle) characteristics. The widely used thickness of the ring mold is 32-127 mm^[12]. The thicker the mold, the deeper is the die and the smaller is the aperture ratio, resulting in greater die wall resistance. In this study, the thickness of the ring mold chosen was 40 mm. Table 2 lists the design specifications of the ring mold.

Table 2 Design specifications of the ring mold

| Inner diameter /mm | Thickness /mm | Aperture /mm | Type | Arrangement |
|--------------------|---------------|--------------|----------|----------------------|
| 360 | 40 | 8 | Straight | Equilateral triangle |

3.2.2 Rollers

Failure of the ring mold is mainly attributed to bending fatigue stress which is caused by alternating loads on the cross section of the ring mold. This fatigue damage is caused by the stress amplitude and stress ratio under alternating loads. Fatigue failure is accelerated when the stress amplitude or the stress ratio increased^[13]. The stress amplitude and the stress ratio are all related to the number of rollers. This research investigated the change of numerical value of the stress amplitude and stress ratio as a function of the number of rollers; we also determined a reasonable number of rollers, so as to improve the service life of the ring mold. The bending moment calculation and distribution of the ring mold are shown on Figure 3.

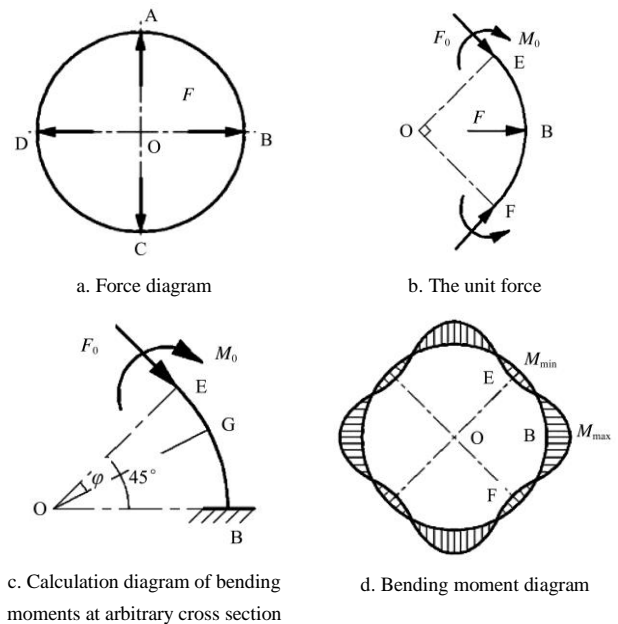


Figure 3 Bending moment calculation and distribution in the ring mold

In Figure 3b, the force and bending moment at cross section E are given as:

$$F_0 = \frac{\sqrt{2}}{2} F \tag{3}$$

$$M_0 = \left(\frac{\sqrt{2}}{2} - \frac{2}{\pi} \right) FR \tag{4}$$

where, *F* is the force between the rollers and the ring mold, kN; *F*₀ is the force at cross section E, kN; *M*₀ is

bending moment at cross section E, kN m; R is inner radius of the ring mold, mm.

In Figure 3c, the bending moment at an arbitrary cross section is given as:

$$M(\varphi) = FR \left(\frac{2}{\pi} - \frac{\sqrt{2}}{2} \cos \varphi \right) \quad (5)$$

In Figure 3d, the biggest bending moment M_{\max} and the smallest bending moment M_{\min} are given as:

$$M_{\max} = FR \left(\frac{2}{\pi} - \frac{1}{2} \right) = 0.137FR \quad (6)$$

$$M_{\min} = FR \left(\frac{2}{\pi} - \frac{\sqrt{2}}{2} \right) = -0.07FR \quad (7)$$

The stress amplitude is given as:

$$\Delta\sigma_4 = \sigma_{\max} - \sigma_{\min} = 0.207 \frac{FR}{W} \quad (8)$$

where, the subscript 4 is the number of rollers; W is bending section modulus of the ring mold, mm⁴.

The stress ratio is given as:

$$s_4 = \frac{\sigma_{\min}}{\sigma_{\max}} = \frac{-0.07FR/W}{0.137FR/W} = -0.511 \quad (9)$$

The same calculations showed that $\Delta\sigma_3$ was $0.216FR/W$ and s_3 was -0.532 , when the number of rollers was 3; $\Delta\sigma_2$ was $0.5FR/W$ and s_2 was -0.572 , when the number of rollers was 2. The results of $\Delta\sigma$ and s showed that $\Delta\sigma_4$ was 1.8% less than $\Delta\sigma_3$, and $\Delta\sigma_2$ was the largest; s_3 was 3.7% less than s_4 , and s_4 was the largest. The lowest stress amplitude was obtained when the number of rollers is 4. Increasing the number of rollers would reduce the diameter of the rollers when the ring mold's diameter was fixed, which would adversely affect the stability and strength of the roller. At the same time, considering that $\Delta\sigma$ is the most important control factor of fatigue damage, our research determined that the reasonable number of rollers was 4.

The roller adopted a grooved surface. The inner diameter of the ring mold D was twice as long as the roller's diameter d_0 . Considering the adjustment of gap and other factors, this relationship is shown in Equation (10)^[14]:

$$d_0 = (0.3-0.5)D \quad (10)$$

The roller diameter affects the production efficiency and the intake angle of biomass particles being pelleted.

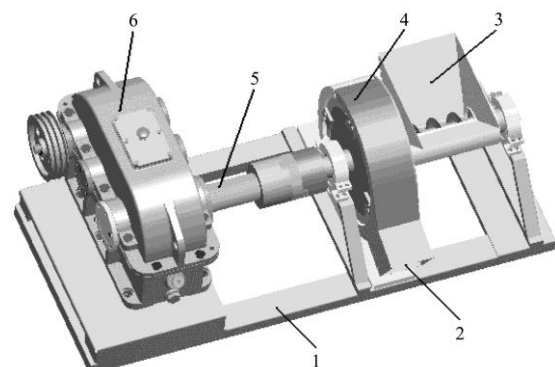
Thus, the roller diameter should be as large as possible. In order to convey the particles more easily from the feed zone to the extrusion zone, the ring mold and the rollers should maintain a certain clearance. Rollers were installed into the ring mold, and were adjusted to slightly contact each other to cause rotation of the rollers. Table 3 lists the design specifications of rollers for the ring mold pelletizer.

Table 3 Design specifications of rollers for the ring mold pelletizer

| Diameter of roller /mm | Depth of groove /mm | Roll thickness /mm | Tolerance clearance /mm |
|------------------------|---------------------|--------------------|-------------------------|
| 120 | 4 | 90 | 0.1 |

3.3 Modeling the ring mold pelletizer

Establishing each of the main working parts of the ring mold pelletizer involved creating each feature surface by way of stretching, rotating, scanning, mixing, shelling and other methods^[15-17]. The assembly modeling module in the Pro/Engineer software was used to complete the virtual assembly. According to the assembly movement and connection of the main working parts, the corresponding relationship and the connection type of setting was selected. Assembly of each part separately was completed first. This was followed by finishing the whole assembly. Lastly, an interference check was performed to ensure that there were no interferences in the whole assembly. The whole model of the ring mold pelletizer is shown in Figure 4.



1. Base 2. Feed outlet 3. Feed inlet 4. Ring mold cover 5. Bearing 6. Gearbox

Figure 4 Whole model of ring mold pelletizer

4 Simulation analysis

4.1 Determination of the interaction force F between rollers and ring mold

The motor provided the energy for the ring mold to rotate through the motion bearing ring connected rigidly

between the ring mold and the motor. In one minute, the energy W' provided by the motor is given in Equation (11):

$$W' = P \times 60 \quad (11)$$

where, P is motor power, kW.

In one minute, the energy required for the ring mold rotation is given in Equation (12):

$$E = Me_h \varphi = Me_h \times 2\pi n \quad (12)$$

where, Me_h is rotating force moment, J; φ is the turning angle of the ring mold in one minute, rad; n is speed of the ring mold, r/min.

The rotating force moment of the ring mold is given in Equation (13):

$$Me_h = \frac{60P \times 1000}{2\pi n} = 9550 \frac{P}{n} \quad (13)$$

The driving force Q to enable the rollers' rotation was the sum of the friction force acting on the surface of the rollers and the friction force produced by the extrusion of materials on the rotating ring mold. The friction force Q' between the materials and the ring mold is equal to the value of Q . By analysis of moments, the ring mold stress can be obtained from Equation (14):

$$\sum M = 0, \quad Me_h - 4Q'R = 0 \quad (14)$$

where, R is inner radius of ring mold, mm.

According to Equations (13) and (14), and knowing that $Q'=Q$, the equation for Q could be written as:

$$Q = 2388 \frac{P}{nR} \quad (15)$$

Meanwhile, the friction force Q between the materials and the rollers is caused by the pressing force F' between the rollers and the materials (which is equal to the pressing force F between the ring mold and the materials, and F is the force between the rollers and the ring mold, F' is equal to F), Q could be written as:

$$Q = \nu F' \quad (16)$$

where, ν is the frictional coefficient between the particles and the pressure rollers, which is 0.35 to 0.40^[12].

According to Equations (15) and (16), and keeping in mind that $F'=F$, F could then be written as:

$$F = 2388 \frac{P}{\nu n R} \quad (17)$$

In this study, P is 12.75 kW, n is 45.4 r/min, R is

180 mm, and ν is 0.38. So, F is equal to 9.8 kN when the number of rollers is four. This value was used to calculate the space torques acting on the screw conveyor.

4.2 Transferring the model into ADAMS

Mechanism/Pro is the interface module which connected the 3D solid modeling software Pro/Engineer and the dynamics simulation analysis software ADAMS^[18-20]. This utility model has the advantage of seamless connection. The assembled model can be transferred into ADAMS and dynamic simulation would be done by means of the Adams solver.

4.3 Simulation analysis

Simulation analysis using Adams/Solver was carried out with input parameters involving the angular velocity of the ring mold's rotation and the spatial force F between the rollers and the ring mold^[21-24]. The main processes of the simulation analysis involved: a) defining the names and materials of the various parts; b) adding the motion pairs and drives; c) checking the model; d) adding the loads; e) running the simulation. The results of simulation analysis on the torques involved as a function of the number of rollers generated by the ADAMS/Postprocessor module are shown in Figure 5. It shows that the ring mold turns 3.03 laps in 4 seconds and is consistent with the actual law of rotation. The maximum space torques acting on the screw conveyor are 1.06×10^6 N mm, 7.80×10^5 N mm and 6.75×10^5 N mm, for four, three and two rollers, respectively. The largest torque resulted from the biggest friction torque for the case of the 4-roller design. The production efficiency of a 4-roller design is about 1.33 times greater than that of the 3-roller design and 2 times that of the 2-roller design. However, the electrical power that is used to drive the 4-roller design is about 1.36 times more than the 3-roller and 1.57 times the 2-roller designs. According to the efficiency and power consumption of the pelletizer, the optimal number of rollers is 4.

5 Fabrication of prototype of the ring mold pelletizer

An actual prototype of the ring mold pelletizer was fabricated to evaluate the design and simulate its working state. The ring mold pelletizer was driven by a 15 kW

power three-phase asynchronous electric motor (Table 1). A reducer was used to decrease the rotating speed of the ring mold and increase the transmitting torque. Transmission ratio of the reducer is 28. Figure 6 shows a photograph of the prototype model of the ring mold pelletizer.

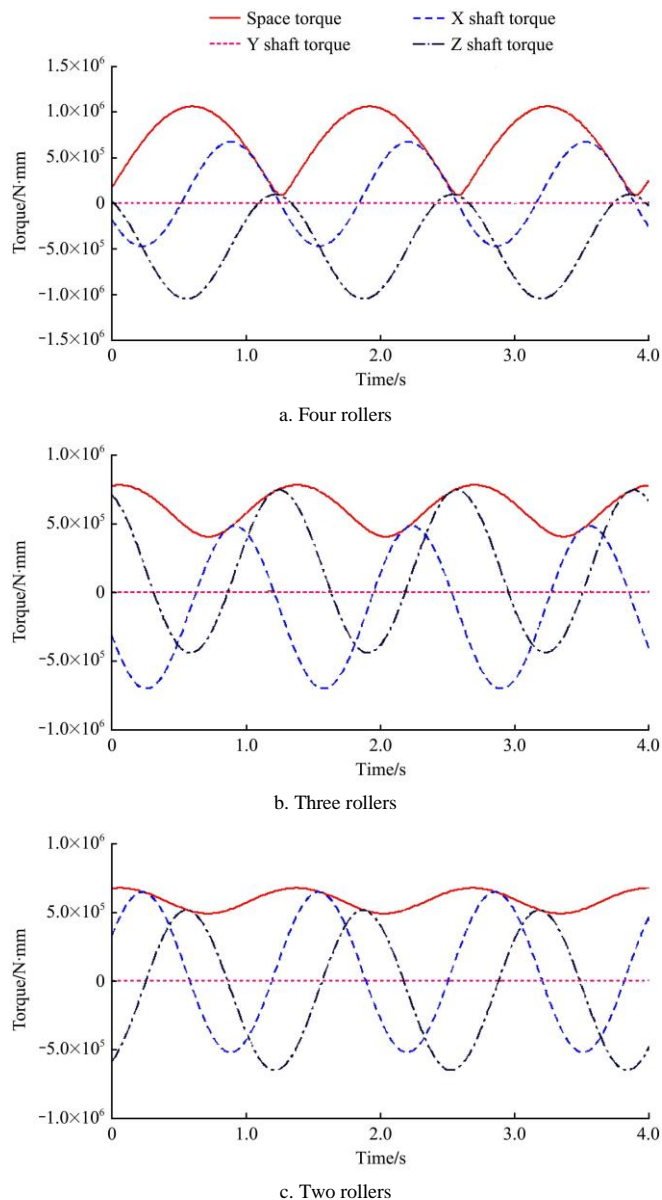


Figure 5 Torque in the screw conveyor as a function of the number of rollers in the design

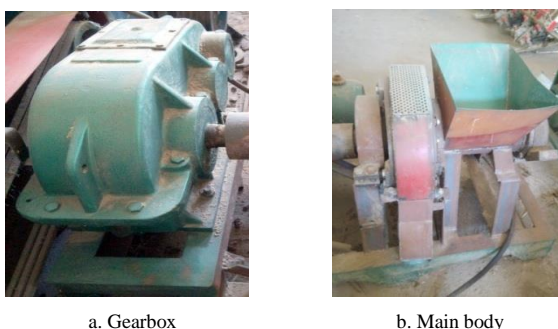


Figure 6 Prototype of the ring mold pelletizer

6 Testing of prototype of the ring mold pelletizer

Past research has shown that pellet durability is the most important physical property as it indicates the resistance of pellets to breakage and disintegration during handling, transport and storage^[25-28]. However, the effect of material and processing variables on pellet durability is not easily quantifiable, especially to the machine operator. The method and pressure of compaction are determined for the specified prototype machine in this study. Pellet durability depends primarily upon the moisture content, particle size and moisture conditioning time of biomass.

6.1 Materials and methods

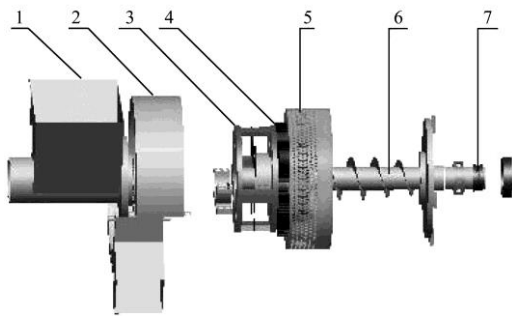
6.1.1 Corn stover samples

Corn stover without cobs was obtained from the experimental farm of Shenyang Agricultural University, Shenyang, China (Lat. 41.8, Long. 123.4) in October 2012. The initial moisture content of ground corn stover was 8.8% wet basis (w.b.); it decreased to 8.1% (w.b.) after it was stored for 6 months in the laboratory.

6.1.2 Pelleting of corn stover

Pelleting tests were conducted using the ring mold pelletizer prototype which was designed based on the Pro/Engineer software^[14]. Corn stover samples with five different particle size intervals (4.76-5.66 mm, 3.36-4.76 mm, 2.38-3.36 mm, 1.41-2.38 mm and 0-1.41 mm), at 10%, 15%, 20%, 25% and 30% (w. b) moisture content, and 2, 3, 4, 5 and 6 h of moisture conditioning time (the samples being sealed into air tight bags for a specific time period) were used.

The ring mold pelletizer was driven by a 15 kW power 3-phase asynchronous electric motor (Shanghai Shenyue Electrical Co., Ltd. Daxi, Wenling, Zhejiang, China). A coupling connected the motor with the spindle of the pelletizer to rotate the ring mold after reducing the speed and increasing the torque with a reducer. Transmission ratio of the reducer was 28. Figure 7 shows the main body of the pelletizer which includes a screw conveyor, ring mold, roller, roll tray and ancillary components.



1. Feed inlet 2. Ring mold cover 3. Roller tray 4. Roller 5. Ring mold
6. Screw conveyer 7. Bearing

Figure 7 Decomposition view of the main body assembly of the ring die pelletizer

The ring mold and rollers compressed the sample particles into a specified shape (pellet) and density. The rotational speed of the ring mold was 0.85 m/s.

6.1.3 Durability determination

According to the European standard (CEN/TS 15210-1-2005)^[13], 100 g of fuel pellets were subjected to free-fall on a hard surface from a height of 1.8 m. Each test was repeated 10 times (pellets). The mass (g) of unbroken fuel pellets m_1 was taken after falling, and the durability DS was calculated using the following equation:

$$DS = \frac{m_1}{m_0} \times 100\% \quad (18)$$

where, m_0 is the total mass of the fuel pellets, g.

6.1.4 Experimental design

Durability of fuel pellets (in sealed bags) was tested 0, 24, 48, 72 and 96 h after they were produced. The regression equation (Equation (19)) shows the effects of moisture content, particle size and moisture conditioning time on the pellet durability of corn stover samples that were determined using the analysis of variance (ANOVA) and response surface methodology (RSM) using the Design Expert software version 7.0 (Stat-Ease Inc., Minneapolis, MN, USA)^[29-32]. The main advantage of the RSM is that it can evaluate multiple parameters and their interactions with a small number of experiments. Hence, RSM was used to optimize the process parameters to maximize the durability of fuel pellets. The parameters studied were moisture content (x_1), particle size (x_2) and moisture conditioning time (x_3). It is assumed that the independent variables affected the response variable. The response variable which is pellet

durability (y) was calculated after the experiment and can be defined as:

$$y = f(x_1, x_2, x_3) \quad (19)$$

The real values and the coded factor levels of the independent variables are given in Table 4.

Table 4 Coded levels for independent variables used in experimentation

| Code | Factor | | |
|------------|--|---------------------------------|--|
| z_j | x_1 (moisture content) /%, w. b. | x_2 (particle size) /mm | x_3 (moisture conditioning time)/h |
| 1.682 | 28.41 | 4.182 | 5.682 |
| 1 | 25 | 3.5 | 5 |
| 0 | 20 | 2.5 | 4 |
| -1 | 15 | 1.5 | 3 |
| -1.682 | 11.59 | 0.818 | 2.318 |
| Δ_j | 5 | 1 | 1 |

The results of this testing is given in the results and discussion, wherein the optimal values of moisture content, screen size (particle size) and moisture conditioning time were identified.

6.2 Results and discussion

Pelleting tests that were carried out in the ring mold pelletizer prototype were replicated thrice and tested for any significant difference from the predicted value (Table 5).

Table 5 Actual value and predicted value acquired from the experiment and Design Expert software, respectively

| Test number | z_1 | z_2 | z_3 | Actual value | Predicted value |
|-------------|--------|--------|--------|--------------|-----------------|
| 1 | -1 | -1 | -1 | 0.9916 | 0.9931 |
| 2 | 1 | -1 | -1 | 0.9966 | 0.9963 |
| 3 | -1 | 1 | -1 | 0.9902 | 0.9892 |
| 4 | 1 | 1 | -1 | 0.9921 | 0.9924 |
| 5 | -1 | -1 | 1 | 0.9929 | 0.9932 |
| 6 | 1 | -1 | 1 | 0.9925 | 0.9927 |
| 7 | -1 | 1 | 1 | 0.9933 | 0.9928 |
| 8 | 1 | 1 | 1 | 0.9932 | 0.9923 |
| 9 | -1.682 | 0 | 0 | 0.9918 | 0.9916 |
| 10 | 1.682 | 0 | 0 | 0.9934 | 0.9938 |
| 11 | 0 | -1.682 | 0 | 0.9971 | 0.9961 |
| 12 | 0 | 1.682 | 0 | 0.9914 | 0.9926 |
| 13 | 0 | 0 | -1.682 | 0.9924 | 0.9921 |
| 14 | 0 | 0 | 1.682 | 0.9916 | 0.9921 |
| 15 | 0 | 0 | 0 | 0.9978 | 0.9976 |
| 16 | 0 | 0 | 0 | 0.9981 | 0.9976 |
| 17 | 0 | 0 | 0 | 0.9969 | 0.9976 |
| 18 | 0 | 0 | 0 | 0.9975 | 0.9976 |
| 19 | 0 | 0 | 0 | 0.9983 | 0.9976 |
| 20 | 0 | 0 | 0 | 0.9968 | 0.9976 |

The Design-Expert 7.0 software was used for analyzing the response surface data. It also optimized the independent variables based on the response variable (pellet durability).

6.2.1 Regression equation

Analysis of variance for the response surface quadratic model for durability is given in Table 6. It is evident that the effects of factors and interactions of these factors are significant except moisture conditioning time.

Table 6 Analysis of variance for the pellet durability as a function of moisture content, particle size and moisture conditioning time using composite design

| Source | Sum of squares | <i>d</i> | Mean square | <i>F</i> value | P-value Prob> <i>F</i> | Significance |
|---|------------------------|----------|------------------------|-----------------------|------------------------|--------------|
| Model | 1.33×10 ⁻⁴ | 8 | 1.66×10 ⁻⁵ | 19.64 | <0.0001 | ** |
| <i>z</i> ₁ | 6.05×10 ⁻⁶ | 1 | 6.05×10 ⁻⁶ | 7.18 | 0.0215 | * |
| <i>z</i> ₂ | 1.52×10 ⁻⁵ | 1 | 1.52×10 ⁻⁵ | 17.97 | 0.0014 | ** |
| <i>z</i> ₃ | 2.18×10 ⁻¹⁰ | 1 | 2.18×10 ⁻¹⁰ | 2.59×10 ⁻⁴ | 0.9875 | |
| <i>z</i> ₁ <i>z</i> ₃ | 6.85×10 ⁻⁶ | 1 | 6.85×10 ⁻⁶ | 8.12 | 0.0158 | * |
| <i>z</i> ₂ <i>z</i> ₃ | 6.13×10 ⁻⁶ | 1 | 6.13×10 ⁻⁶ | 7.26 | 0.0208 | * |
| <i>z</i> ₁ ² | 4.31×10 ⁻⁵ | 1 | 4.31×10 ⁻⁵ | 51.06 | <0.0001 | ** |
| <i>z</i> ₂ ² | 1.89×10 ⁻⁵ | 1 | 1.89×10 ⁻⁵ | 22.41 | 0.0006 | ** |
| <i>z</i> ₃ ² | 5.43×10 ⁻⁵ | 1 | 5.43×10 ⁻⁵ | 64.36 | <0.0001 | ** |
| Residual | 9.28×10 ⁻⁶ | 11 | 8.43×10 ⁻⁷ | | | |
| Lack of Fit | 7.36×10 ⁻⁶ | 6 | 1.23×10 ⁻⁶ | 3.21 | 0.1109 | |
| Pure Error | 1.91×10 ⁻⁶ | 5 | 3.83×10 ⁻⁷ | | | |
| Correlation total | 1.42×10 ⁻⁴ | 19 | | | | |

Note: “*” significant difference at *P*<0.05 level; “***” means significant difference at *P*<0.01 level; *z*₁ is coded level for moisture content; *z*₂ is coded level for particle size; *z*₃ is coded level for moisture conditioning time.

The regression equation obtained for the model of the second degree in terms of coded factors is:

$$y = 0.9976 + 0.000666z_1 - 0.00105z_2 + 0.000004z_3 - 0.000925z_1z_3 + 0.000875z_2z_3 - 0.00173z_1^2 - 0.00115z_2^2 - 0.00194z_3^2 \quad (20)$$

where, *y* is pellet durability; *z*₁ is coded level for moisture content; *z*₂ is coded level for particle size; *z*₃ is coded level for moisture conditioning time.

The relationship between the real values and the coded factor levels of the independent variables are given in Equation (21).

$$x_i = z_i\Delta_i + \bar{x}_i, \quad (i = 1, 2, 3) \quad (21)$$

According to Table 5 and Equations (20) and (21), the regression equation of the pellet durability with the real values of moisture content, particle size and moisture conditioning time was calculated using the following equation:

$$y = 0.926 + 0.00364x_1 + 0.00117x_2 + 0.017x_3 - 0.000185x_1x_3 + 0.000875x_2x_3 - 0.0000691x_1^2 - 0.00115x_2^2 - 0.00194x_3^2 \quad (22)$$

where, *y* is pellet durability; *x*₁ is moisture content, %; *x*₂ is particle size, mm; *x*₃ is moisture conditioning time, h.

6.2.2 Optimization of process conditions

According to Equations (21) and (22), the maximum pellet durability is 99.79%, and the maximum points are given in Equation (23).

$$\begin{aligned} x_{1,o} &= 0.24 \times 5 + 20 = 21.2 \\ x_{2,o} &= -0.53 \times 1 + 2.5 = 1.97 \\ x_{3,o} &= -0.18 \times 1 + 4 = 3.82 \end{aligned} \quad (23)$$

where, *x*_{1,0} is optimized variable of moisture content, %; *x*_{2,0} is optimized variable of particle size, mm; *x*_{3,0} is optimized variable of moisture conditioning time, h.

Thus, the optimized variables are: moisture content of 21.2% w.b., particle size of 1.97 mm and moisture conditioning time of 3.82 h.

7 Conclusions

This research analyzed the forming process of fuel pellets using a ring mold pelletizer. The following conclusions can be drawn:

1) The effects of stress amplitude and the stress ratio on the fatigue failure in conditions of 4-, 3-, and 2-roller designs were investigated. The optimal number of rollers in the ring mold pelletizer was 4.

2) Pro/Engineer software was used to create a 3D solid model of ring mold pelletizer and Adams software was used for simulation to determine the space torque between the screw conveyer and the ring mold. The simulation results validated that 4-roller design was more reasonable than the 3- or 2-roller design.

3) The material of the ring mold was high chromium alloy steel with a thickness of 40 mm and an inner diameter of 360 mm. The die holes were arranged as equilateral triangle, the hole was straight and the diameter was 8 mm. The roller has a grooved surface structure with a thickness of 90 mm and diameter of 120 mm. The depth of groove was 4 mm and the tolerance clearance was 0.1 mm. The ring mold pelletizer was powered by a 15 kW three-phase asynchronous electric motor.

4) Pellets formed in the ring mold pelletizer using corn stover had acceptable durability according to European standards.

5) Particle size and moisture content significantly affected the pellet durability of corn stover.

6) Pellets manufactured using the ring mold pelletizer had an optimized pellet durability of 99.79% at a particle size of 1.97 mm, moisture content of 21.2% w.b. and moisture conditioning time of 3.82 h.

Acknowledgements

The authors would like to express their gratitude for the financial support received from the China Scholarship Council (201308210283), the national Spark Program (2015GA650012), the Cultivation Plan for Youth Agricultural Science and Technology Innovative Talents of Liaoning Province (2014053) and the funding provided by Youth Fund of Shenyang Agricultural University (20121002). Funding support from BioFuelNet Canada (BFN) is also acknowledged.

Nomenclature

| | |
|----------------|---|
| α | angle of extrusion forming zone, rad |
| β | angle of whole compression deformation zone, rad |
| i | transmission ratio |
| n_s | rotational speed of spindle, r/min |
| n_m | rotational speed of the motor, r/min |
| D | inner diameter of ring mold, mm |
| v | line speed of ring mold, mm/s |
| F | force between rollers and ring mold, kN |
| F_0 | force at cross section of E, kN |
| M_0 | bending moment at cross section of E, kN m |
| M_φ | bending moment at arbitrary cross section, kN m |
| $\Delta\sigma$ | stress amplitude, MPa |
| s | stress ratio |
| W | bending section modulus of ring mold, mm ⁴ |
| d_0 | diameter of roller, mm |
| W' | one minute energy provided by motor, kWh |
| P | motor power, kW |
| Me_h | rotating force moment, J |
| φ | turning angle of ring mold in one minute, rad |
| n | rotational speed of ring mold, r/min |
| Q | driving force to enable rollers' rotation, kN |

| | |
|-------|--|
| Q' | friction force between materials and ring mold, kN |
| F' | pressing force between rollers and materials, kN |
| ν | frictional coefficient between materials and rollers |
| R | inner radius of ring mold, mm |

[References]

- [1] Karkania V, Fanara E, Zabaniotou A. Review of sustainable biomass pellets production – A study for agricultural residues pellets' market in Greece. *Renewable and Sustainable Energy Reviews*, 2012; 16(3): 1426–1436. doi:10.1016/j.rser.2011.11.028.
- [2] Adapa P K, Tabil L G, Schoenau G J. Factors affecting the quality of biomass pellet for biofuel and energy analysis of pelleting process. *Int J Agric & Biol Eng*, 2013; 6(2): 1–12. doi: 10.3965/j.ijabe.20130602.001.
- [3] Qiu G Q. Testing of flue gas emissions of a biomass pellet boiler and abatement of particle emissions. *Renewable Energy*, 2013; 50: 94–102. doi: 10.1016/j.renene.2012.06.045.
- [4] Rabaçal M, Fernandes U, Costa M. Combustion and emission characteristics of a domestic boiler fired with pellets of pine, industrial wood wastes and peach stones. *Renewable Energy*, 2013; 51(3): 220–226. doi: 10.1016/j.renene.2012.09.020.
- [5] Wang J C, Dai L, Tian Y S. Analysis of the development status and trends of biomass energy industry in China. *Transactions of the CSEA*, 2007; 23(9): 276–282. doi: 10.3321/j.issn:1002-6819.2007.09.053. (in Chinese with English abstract)
- [6] Kim S, Dale B E. Global potential bioethanol production from wasted crops and crop residues. *Biomass & Bioenergy*, 2004; 26(4): 361–375. doi: 10.1016/j.biombioe.2003.08.002.
- [7] Iroba K L, Tabil L G, Sokhansanj S, Meda V. Producing durable pellets from barley straw subjected to radio frequency-alkaline and steam explosion pretreatments. *Int J Agric & Biol Eng*, 2014; 7(3): 68–82. doi: 10.3965/j.ijabe.20140703.009.
- [8] Wang H, Lu P, Wu Y Y, Du H G. Life study of biomass loop die based on COSMOS. *Journal of Agricultural Mechanization Research*, 2011; 33(8): 193–196. doi: 10.3969/j.issn.1003-188X. 2011. 08.049. (in Chinese with English abstract)
- [9] Liu B C, Liang X M, Guo H Y. Analysis of biomass briquette machine ring mold length-diameter ratio of finite element based on ANSYS. *Key Engineering Materials*, 2012; 501(1): 463–466. doi: 10.4028/www.scientific.net/KEM.501.463.
- [10] Abubakre O K, Garba A B, Tukur H. Design and

- fabrication of model feed pelletizer. *Applied Mechanics and Materials*, 2014; 533(2): 64–67. doi: 10.4028/www.scientific.net/AMM.533.64.
- [11] Tu D Y, Wang X, Xu A H. Virtual design and simulation for biomass plane-die briquetting machine. *Advanced Materials Research*, 2011; 347–353(10): 2432–2437. doi: 10.4028/www.scientific.net/AMR.347-353.2432.
- [12] Huo L L, Hou S L, Tian Y S. Wear failure analysis on roller assembly of biomass pellet mill. *Transactions of the CSAE*, 2010; 26(7): 102–106. doi: 10.3969/j.issn.1002-6819.2010.07.018 (in Chinese)
- [13] Solid biofuels-Methods for the determination of mechanical durability of pellets and briquettes-Part1: Pellets. German Version CEN/TS 15210-1. 2005.
- [14] Gao W. Digital design and experiment study on biomass pelletizer of granular burning stove. PhD dissertation. Shenyang: Shenyang Agricultural University. 2012. (in Chinese)
- [15] Gecevaska V, Cus F, Dukovski V. Modelling of manufacturing activities by process planning knowledge representation. *International Journal of Simulation Modelling*, 2006; 5(2): 69–81. doi: 10.2507/IJSIMM05(2)3.062.
- [16] David W, Porter A, Bruce P. Data fusion modeling for groundwater systems. *Journal of Contaminant Hydrology*, 2000; 42: 303–335. doi: 10.1016/S0169-7722(99)00081-9.
- [17] Vinodh S, Sundararaj G, Devadasan S R. Agility through rapid prototyping technology in a manufacturing environment using a 3D printer. *Journal of Manufacturing Technology Management*, 2009; 20(7): 1023–1041. doi: 10.1108/17410380910984267.
- [18] Khan S, Shah K, Izhar U H, Khan H, Ali S, Ahmad N, et al. Observation of the starting and low speed behavior of small horizontal axis wind turbine. *Journal of Wind Energy*, 2014; (2014): 1–8. doi: 10.1155/2014/527198.
- [19] Katz R, Li Z. Kinematic and dynamic synthesis of a parallel kinematic high speed drilling machine. *International Journal of Machine Tools and Manufacture*, 2004; 44(12-13): 1381–1389. doi: 10.1016/j.ijmactools.2004.04.007.
- [20] Parametric Technology Corporation. Pro/ENGINEER Wildfire 2.0 Pro/TOOLKIT User's Guide. USA, PTC. 2004.
- [21] Zhang X J, Wu C W, Wang X D. Motion simulation and analysis of separating sieve mechanism for scrap plastic firm. *Transactions of the CSAE*, 2007; 23(7): 113–116. doi: 10.3321/j.issn:1002-6819.2007.07.022. (in Chinese with English abstract)
- [22] Braun T, Christmann D, Gotzhein R, Igel A, Kuhn T. Virtual prototyping of distributed embedded systems with feral. *International Journal of Modelling and Simulation*, 2014; 34(2): 91–101. doi: 10.2316/Journal.205.2014.2.205-5968.
- [23] Sinou J J. Transient non-linear dynamic of automotive disc brake squeal-on the need to consider both stability and non-linear analysis. *Mechanics Research Communications*, 2010; 37(1): 96–105. doi: 10.1016/j.mechrescom.2009.09.002.
- [24] Stubkier S, Pedersen H C, Jonkman J M. Analysis of load reduction possibilities using a hydraulic soft yaw system for a 5-MW turbine and its sensitivity to yaw-bearing friction. *Engineering Structures*, 2014; 69: 123–134. doi:10.1016/j.engstruct.2014.01.022.
- [25] Tabil L G. Binding and pelleting characteristics of alfalfa. Unpublished PhD dissertation. Canada, Saskatoon: University of Saskatchewan, 1996.
- [26] Chin O C, Siddiqui K M. Characteristics of some biomass briquettes prepared under modest die pressures. *Biomass & Bioenergy*, 2000; 18: 223–228. doi: 10.1016/S0961-9534(99)00084-7.
- [27] Kashaninejad M, Tabil L G, Knox R. Effect of compressive load and particle size on compression characteristics of selected varieties of wheat straw grinds. *Biomass & Bioenergy*, 2014; 60: 1–7. doi: 10.1016/j.biombioe.2013.11.017.
- [28] Al-Widyan M I, Al-Jalil H F, bu-Zreig M M, Abu-Hamdeh N H. Physical durability and stability of olive cake briquettes. *Canadian Biosystems Engineering*, 2002; 44: 3–41. doi: 10.1016/S0196-8904(01)00064-4.
- [29] Lu D H, Tabil L G, Wang D C, Wang G H, Wang Z Q. Optimization of binder addition and compression load for pelletization of wheat straw using response surface methodology. *Int J Agric & Biol Eng*, 2014; 7(6): 67–78. doi:10.3965/j.ijabe.20140706.009.
- [30] Karunanithy C, Muthukumarappan K. Influence of extruder and feedstock variables on torque requirement during pretreatment of different types of biomass) – A response surface analysis. *Biosystems Engineering*, 2011; 109(1): 37–51. doi: 10.1016/j.biosystemseng.2011.02.001.
- [31] Goyal R K, Vishwakarma R K, Wanjari O D. Optimisation of the pigeon pea dehulling process. *Biosystems Engineering*, 2008; 99: 56–61. doi: 10.1016/j.biosystemseng.2007.09.015.
- [32] Altemimi A, Watson D G, Kinsel M, Lightfoot D A. Simultaneous extraction, optimization, and analysis of flavonoids and polyphenols from peach and pumpkin extracts using a TLC-densitometric method. *Chemistry Central Journal*, 2015; 9: 39–54. doi: 10.1186/s13065-015-0113-4.